Boletim da Sociedade Astronômica Brasileira, **35**, no. 1, 211-214

Observational study of the polar cataclysmic variable candidate CRTS J091936.6−055519

N. Palivanas[9], A. S. Oliveira[9], C. V. Rodrigues[2], D. C. Souza[9], I. J. Lima[3], K. M. G. Silva[4], M. S. Palhares[9], & M. Martins[9]

[1] Universidade do Vale do Paraíba, São José dos Campos, Brasil e-mail: natalia.palivanas@alumni.usp.br, alexandre@univap.br, diegocarvalhodesouza@hotmail.com, matheus_spalhares@hotmail.com, prof.murilomartins@gmail.com
[2] Instituto Nacional de Pesquisas Espaciais, São José dos Campos, Brasil e-mail: claudiavilega@gmail.com
[3] CONICET-Universidad de Buenos Aires, Argentina e-mail: isabellima01@gmail.com
[4] Gemini Observatory, Chile e-mail: karleyne@gmail.com

Abstract. We present the characterization of CRTS J091936.6−055519, a hitherto little studied polar cataclysmic variable selected from an exploratory spectroscopy study of candidates extracted from the CRTS photometric transient catalog. We used spectroscopic and polarimetric data acquired, respctively, at the SOAR and Pico dos Dias observatories, as well as photometry from TESS. The periodicity analysis revealed an orbital period of $P_{orb} = 0.078100 \pm 0.000002$ d, previously unknown. The data show features compatible with a polar cataclysmic variable. The spectra is dominated by the accretion region, featuring multiple-component Hβ and He II emission lines with radial velocity modulated by the P_{orb}. Furthermore, the polarimetry data show the presence of circular and linear polarization, although at low levels compared to most of known polars.

Resumo. Apresentamos o trabalho de caracterização da CRTS J091936.6−055519, uma variável cataclísmica polar, até então pouco estudada, selecionada de estudos de espectroscopia exploratória de candidatas a variáveis cataclísmicas extraídas do catálogo de transientes fotométricos do CRTS. Utilizamos dados de espectroscopia e polarimetria obtidos, respectivamente, nos observatórios SOAR e Pico dos Dias, bem como fotometria obtida pelo TESS. A análise de periodicidade revelou um período orbital de $P_{orb} = 0.078100 \pm 0.000002$ d, até então desconhecido. Os dados mostram características compatíveis com uma variável cataclísmica polar. O espectro é dominado pela região de acreção, com linhas de emissão de Hβ e He II formadas por mais de uma componente e velocidade radial modulada pelo P_{orb}. Os dados de polarimetria mostram a presença de polarização circular e linear, ainda que em níveis baixos comparados aos da maioria das polares conhecidas.

Keywords. binaries (including multiple): close – Techniques: photometric – Techniques: polarimetric

1. Introduction

Cataclysmic Variables (CVs) are semi-detached binary systems composed of a white dwarf (WD) and a red dward (RD) mass donnor. CVs are classified as non-magnetic or magnetic (mCVs), while the latter is usually classified between polars and intermediate polars (IPs). The stream of matter in mCVs is partially or fully dominated by the magnetic field lines of the WD and accumulates onto one or more accretion column near one or both magnetic poles. Unlike IPs and non-magnetic CVs, polars are synchronous systems, i.e., its orbital period is coupled to the rotation period of the WD. While the vast majority of known CVs have orbital periods between 78 min and 12 h, the polars are concentrated below 5 h (Ferrario, Martino & Gänsicke (2015)).

As a consequence of non-periodic variations of the mass-transfer rate ($\dot{M}$), the CVs manifest different brightness states. During high mass-transfer rates (increased $\dot{M}$), the luminosity of a polar mCV is dominated by the accretion column, with intense soft X-ray and cyclotron emissions in visible and IR bands, and featuring He I, He II and Balmer emission lines, with the notable presence of a He II 4686 Å emission line as intense as the Hβ line.

There are still challenges in understanding the origin of the magnetic fields of mCVs, since the ratio of mCVs among the known CVs within a radius of 150 pc is greater than the observed in the population of their progenitors (Pala et al. (2020); Liebert et al. (2015)). Many efforts are being made to increase the sample of well known mCVs in order to unravel their diversity and constrain the possible models, since the evolution of a CV is closely linked to its magnetic field and orbital period. Particularly, Oliveira et al. (2017) initiated a series of spectroscopy observations of mCVs candidates selected mostly from the Catalina Real-Time Transient Survey (Drake et al. (2009)). The spectrum of CRTS J091936.6−055519 (=CSS0919−05), the object of study of this work, was obtained as a part of this exploratory mission and presented in Oliveira et al. (2020). As also observed by Drake et al. (2014), CSS0919−05 have spectral features that match a polar mCV, but other key characteristics such as orbital period, light curve and polarization remained unknown.

2. CSS0919−05

Over the last years, CSS0919−05 was observed by the Catalina Sky Survey (CSS) as a part of the Catalina Real-Time Transient Survey (CRTS), by All-Sky Automated Survey for Supernovae (ASAS-SN) (Kochanek et al. (2017); Shappee et al. (2014)), and by the Zwicky Transient Facility (ZTF) (Masci et al. (2018)). Also, there is a set of unfiltered photometric data made available by The American Association of Variable Star Observers (AAVSO).

Fig. 1 shows the light curves in different optical bands. While ZTF has a limiting magnitude down to ∼20 mag in all filters, CSS is limited to approximetly V∼19.5 mag, and ASAS-SN to V∼17 mag. There are non-periodic brightness states among data

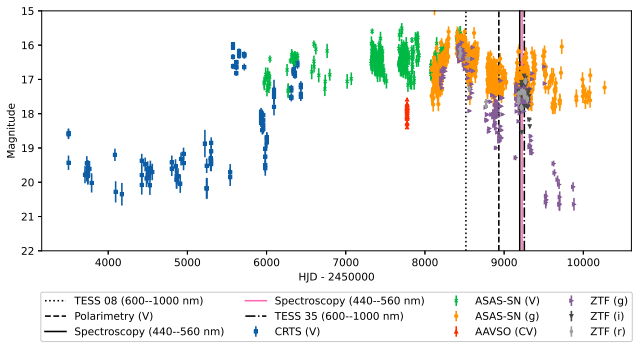

Figure 1. Light curves of CSS0919−05 in different optical bands, where CV refers to unfiltered reduced to V sequence. The vertical lines mark the dates when each of the datasets used in this work was acquired.

from the same survey with rapid variations smaller than 1 mag. The vertical lines mark the date when the data used in this work were acquired.

There is no redshift in the spectra obtained by Drake et al. (2014) and Oliveira et al. (2020). Using Gaia EDR3 data, Bailer-Jones et al. (2021) estimated that CSS0919−05 is at a distance of $d = 438^{+23}_{-26}$ pc, thus confirming the Galactic origin of the target.

3. Observational data and analysis

3.1. Photometry

The Transiting Exoplanet Survey Satellite (TESS) was primary designed to carry out a photometric survey of the sky in the 600–1000 nm band in search for exoplanetary transits in F5 to M5 stars near the Solar System (Ricker et al. (2014)). TESS surveys sectors of 24° × 96° during approximately 27 days with a temporal resolution that ranges from 20 s to 30 min. Its data products are made publicly available by MAST[1] (Mikulski Archive for Space Telescopes) and includes light curves computed by the Science Processing Operations Center (SPOC) for selected objects, as well as Full Frame Images (FFIs) from all sectors. Given its temporal span and resolution, TESS provides promissing data for analysis of variable phenomena such as CVs.

At the time of this work, CSS0919−05 had been observed between February 02 – 27, 2019 (sector 08), and February 09 to March 06, 2021 (sector 35), both available as FFIs only. We used the Python package Lightkurve (Lightkurve Collaboration (2018)) to download, plot and extract the light curves from the FFIs. The 11×11 pixels cutout from sector 08 in Fig 2 shows the field around the Gaia position of CSS0919−05 (marked with a cross) and objects brighter than 21 Gaia Gmag.

We selected a pixel mask to account for the target flux in the FFIs, which was then subtracted by the median flux of the sky. Fig. 3 shows the resulting normalized light curve from sector 08. The gaps correspond to intervals for data transmission or points excluded for being flagged as defective.

We determined the orbital period using the Lomb-Scargle algorithm (Scargle (1982)), a method based on the discrete Fourier transform for periodicity analysis of data with irregular intervals (VanderPlas (1982)) that results in a frequency power spectrum (Fig. 4). In this case, the orbital period of CSS0919−05 is associated with the highest peak of the periodogram, corresponding to $P_{orb} = 0.078100 \pm 0.000002$ d. The

[1] Available online at `https://archive.stsci.edu`

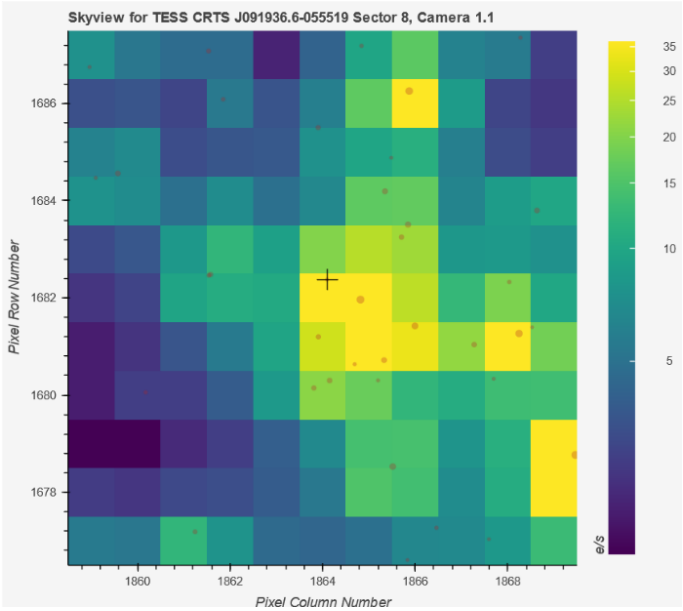

Figure 2. Sector 08 FFI 11×11 pixel cutout centered on the CSS0919−05 Gaia position (cross). The circles mark the Gaia position of objects brighter than 21 Gmag and have radii proportional to their brightness.

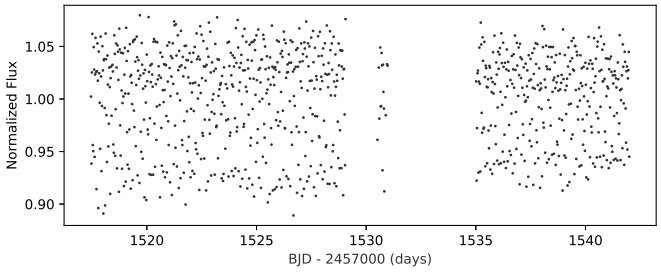

Figure 3. CSS0919−05 normalized light curve from TESS sector 08. The missing data corresponds to flagged points or data transfer intervals.

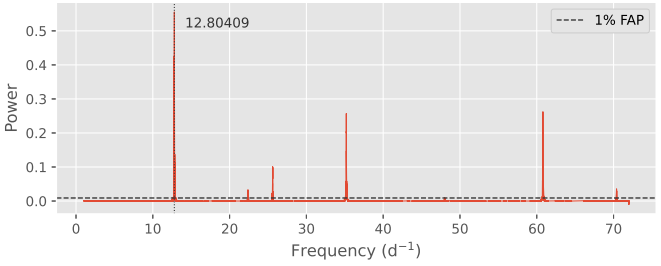

Figure 4. Periodogram calculated using both CSS0919−05 light curves from TESS sectors 08 and 35. The horizontal line marks the height for a 1% false alarm probability level.

horizontal dashed line marks the height for a 1% false alarm probability level.

Due to TESS plate scale of 21″ pixel^{-1}, we used the Python package TESS Localize (Higgins & Bell (2022)), that calculates the position of a signal with a given frequency with a precision up to 1/5 pixel, assuming there is no nearby indistinguishable variable sources. In both sectors, TESS Localize confirmed that

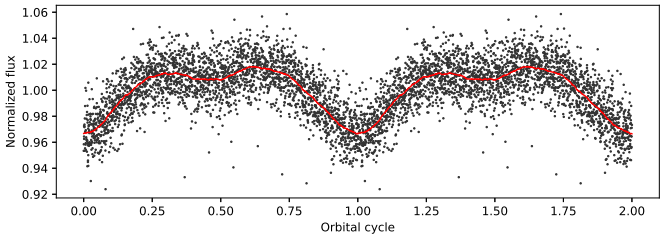

Figure 5. CSS0919−05 period-fold light curve from TESS sector 35. The solid curve is a Savitzky–Golay smoothing filter curve.

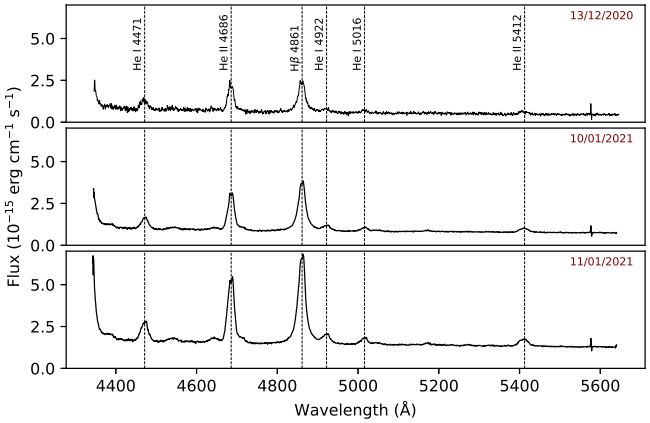

Figure 6. CSS0919−05 average spectra from each night obtained at SOAR. The vertical dashed lines mark the rest wavelength of the observed emission lines.

the position of the periodic signal with P_{orb} matches the target Gaia position.

We then calculated a photometric ephemeris for CSS0919−05, given by Eq. 1, using P_{orb} and an instant of minimum brightnes as reference:

$$T_{phot}\,(BJD) = 2\,459\,255.827\,(5) + 0,078100\,(2) \times E \qquad (1)$$

Fig. 5 shows the period-fold light curve of sector 35, where the solid curve was calculated by a Savitzky–Golay smoothing filter. The perio-fold light curves from both sectors have a profile of a non-eclipsing diskless binary system, and are modulated by the P_{orb}, with a deeper primary minimum followed by a shallow secondary minimum shifted by half an orbital cycle.

3.2. Spectroscopy

Spectroscopic data of CSS0919−05 was obtained between 2020 and 2021 at the SOAR 4.1 m telescope coupled to the Goodman High Throughput Spectrograph (Clemens, Crain & Anderson (2014)), and reduced using standard procedures in IRAF (Tody (1986)). Fig. 6 shows the average spectra from each night with a resolution of 0.62 Å pixel^{-1}. We also measured the central wavelenght of the teluric emission line O I 5577 Å and calculated its radial velocity (which, as it is a line associated with the Earth's atmosphere, should remain as close as possible to zero).

Within the observed wavelength range, all spectra show He I, He II and Hβ emission lines superimposed on a flat continuum. The morphology of the most intense lines varies throughout each night, having up to two peaks in some of the spectra. To track this variation, we adjusted the He II 4686 Å and Hβ lines to a combination of two Lorentz profiles (Fig. 7) and calculated the radial velocity of the central wavelength of each component relative to the rest wavelength of the emission. The resulting radial velocity period-fold curves, shown in Fig. 8, are modulated by P_{orb}. There is an apparent phase-lag between the components, as well as a diference between the hamplitude of the sinusoidal fit and the systemic velocity γ, suggesting these lines originate from more than one structure in the binary system. The Lomb-Scargle analysis of the radial velocities results in an orbital period in agreement with the P_{orb} obtained with TESS data, but with less precision.

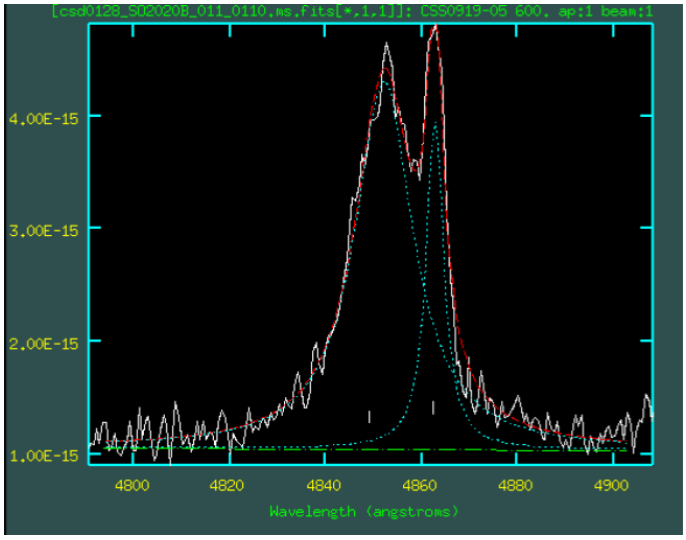

Figure 7. Two-component fitting of the Hβ emission line of one of the CSS0919−05 spectra.

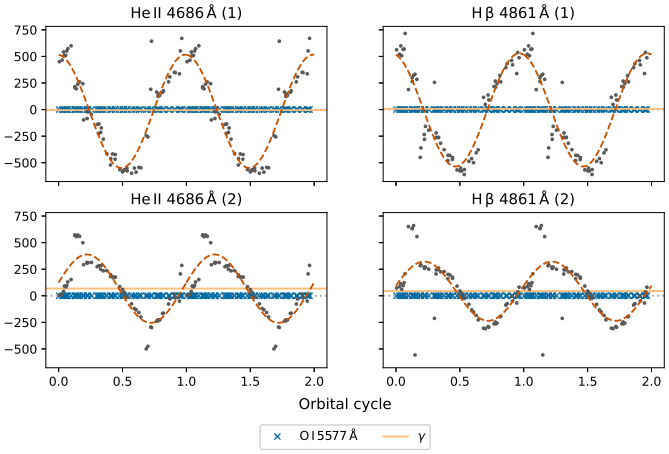

Figure 8. Period-fold radial velocity of two Lorentz components (1 and 2) adjusted to He II 4686 Å and Hβ emission lines from CSS0919−05 spectra. The crosses mark the radial velocity of the O I 5577 Å teluric line, the dashed line is the sinusoidal fit of the radial velocity and the solid horizontal line corresponds to the systemic velocity γ.

3.3. Polarimetry

During March 24 and 26, 2020, CSS0919−05 V-band circular and linear polarization data were obtained at the 1.6 m Perkin-Elmer telescope at the Pico dos Dias Observatory coupled to the IAGPOL polarimetric module (Magalhães (1996)).

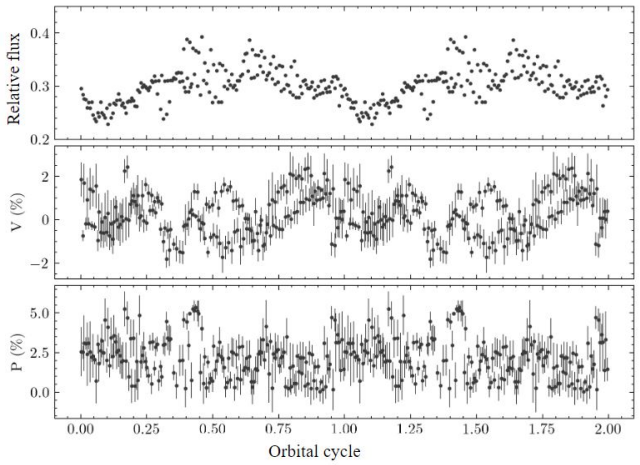

Figure 9. Period-fold relative flux, circular (V) and linear (P) polarization curve of CSS0919−05 in March 26, 2020.

Unfortunately, clouds and high seeing on both nights compromised the data quality specially on the first night, during which less than one orbital cycle was observed. Data reduction was done using standard IRAF tasks and PCCDPACK (Quirós (2000)), a set of CL-IRAF routines for polarimetry analysis. This technique also provides the relative flux of the target, which is computed from the differential photometry of the sum of the fluxes of the ordinary and extraordinary beams separated by the polarimetric module in relation to a comparison objec.

Fig. 9 shows the period-fold circular (V) and linear (P) polarization curve, and the relative flux, obtained on the second night. The circular polarization varies between −2 % and +2 %, while the linear polarization remains below 5 %. Although these are low values compared to those observed in most polars (V∼10 %), there are precedents for cases of polars with low polarization (Schmidt & Stockman (2001); Buckley & Shafter (1995)). However, we don't rule out that this variation is related to light curve flickering (a fast stochastic variation present in accreting systems). The relative flux seems modulated by the orbital cycle.

4. Conclusion

We carried out an analysis to characterize CRTS J091936.6−055519, a polar cataclysmic variable candidate. For this, we used photometry, spectroscopy and polarimetry data obtained, respectively, by TESS, SOAR and Observatório Pico dos Dias.

Using the Lomb-Scargle method with TESS data, we determined the orbital period of $P_{orb} = 0.078100 \pm 0.000002$ d. The period-fold TESS light curve is modulated by P_{orb}, and is compatible with a diskless non-eclipsing polar, featuring a main deeper minimum followed by a shallow valley half an orbital cycle later.

The long-term light curves obtained by CRTS, AAVSO, ASAS-SN and ZTF surveys reveal non-periodic low and high brightness states in different optical bands, from 16 to 21 mag, accompanied by rapid variations smaller than 1 mag.

The spectra between 4400–5600 Å are compatible with that observed in known polars during a high mass-transfer rate state. It is dominated by the accretion column, with Hβ, He I, He II emission lines over a flat continuum, with no evidence of absorption lines. The behavior of the multiple-components lines throughout the observation nights suggests emission by more than one region in the binary system. The orbital modulation, phase-lag and systemic velocity between the period-fold radial velocity of two components adjusted to the most intense emission lines reinforce this hypothesis.

Although the circular polarization have a low value that could be associated with flickering, it wouldn't be the first known case. Since much of the polarization data has been compromised by unfavorable weather conditions, we have plans for new observations. Nevertheless, the other observational characteristics presented in this work indicate the classification of CSS0919−05 as a polar mCV.

Acknowledgements. NP thanks support from Coordenação de Aperfeiçoamento de Pessoal de Nível Superior (CAPES). ASO acknowledges São Paulo Research Foundation (FAPESP) for financial support under grant #2017/20309-7. We acknowledge with thanks the variable star observations from the AAVSO International Database contributed by observers worldwide and used in this research. This work includes data collected by the TESS mission. Funding for the TESS mission is provided by the NASA's Science Mission Directorate. The CSS survey is funded by the National Aeronautics and Space Administration under Grant No. NNG05GF22G issued through the Science Mission Directorate Near-Earth Objects Observations Program. The CRTS survey is supported by the U.S. National Science Foundation under grants AST-0909182. This research made use of Lightkurve, a Python package for Kepler and TESS data analysis (Lightkurve Collaboration, 2018).

References

Bailer-Jones, C. A. L., Rybizki, J., Fouesneau, M., Demleitner, M., & Andrae, R., 2021, VizieR Online Data Catalog, I-352
Buckley, D. A. & Shafter, A. W., 1995, MNRAS, 275, L61
Clemens, J. C., Crain, J. A., Anderson, R., 2014, Ground-based Instrumentation for Astronomy, 5492, 331
Drake, A. et al., 2009, ApJ, 696, 870
Drake, A. J, et al, 2014, ApJ Supplement Series, 213, 9
Ferrario, L., de Martino, D. & Gänsicke, B. T., 2015, SSR, 191, 111
Higgins, M. E. & Bell, K. J. 2022, AAS Journals (submitted); arXiv:2204.06020
Kochanek, C. et al., 2017, PASP, 129.980, 104502
Liebert J., et al., 2015, ApJ, 804, 93
Lightkurve Collaboration, 2018, Astrophysics Source Code Library
Magalhães, A. et al., 1996, ASP Conference Series, 97, 118
Masci, F. J., Laher, R. R., Rusholme, B., et al. 2018, PASP, 131, 995
Oliveira, A. S., et al., 2017, AJ, 153, 144
Oliveira A. S. et al., 2020, AJ, 159, 114
Pala A. F. et al., 2020, MNRAS, 494, 3799
Quirós, A. A. P., 2000, Doctoral thesis, Universidade de São Paulo
Ricker G. R. et al., Journal of Astronomical Telescopes, Instruments, and Systems, 1, 014003
Scargle, J. D., 1982, ApJ, 263, 835
Schmdit, G. D. & Stockman, H., 2001, ApJ, 548, 410
Shappee B. J., Prieto J. L., Grupe D., Kochanek C. S., Stanek K. Z., De Rosa G., Mathur S., et al., 2014, ApJ, 788, 48
Tody, D., 1986, SPIE Instrumentation in astronomy VI, 627, 733
VanderPlas, 2018, ApJ Supplement Series, 236, 16